Remediation of Contaminated Soil with Diesel by Soil Venting Technique

Youngcheol Joo*, Artemiy Fotinich and Vijay K. Dhir****

(*Received January 14, 1998*)

Soil venting is an effective and widely used method to remediate soils contaminated with hydrocarbons. A set of experiments was conducted in a one-dimensional soil column test section to investigate the effect of preheating the air in a soil venting system. Diesel fuel, which was used as the only contaminant, was analyzed and modeled with 14 major components. Temperature readings from the thermocouples located in the test section were recorded during the experiment and the composition of hydrocarbons in the effluent air was also monitored. The results show that the diesel components are removed according to their volatility with the higher volatility components being removed first. An increase in venting air flow rate or inlet air temperature can considerably speed up the process. The increase in inlet air temperature is very effective in increasing the removal rate of the heavier components. A one-dimensional, non-isothermal, complete mixing model was used to predict the evaporation rates of the contaminant components and temperature distribution in the test section. Model results have been found to be in good agreement with the experimental data.

Key Words: Soil Venting Technique, Diesel, Remediation of Soil, Heated Air.

1. Introduction

Contamination of soil and ground water due to underground hydrocarbon spills poses a strong environmental threat. Contaminants enter the subsurface from many sources including leaking storage tanks, ruptured pipelines, chemical waste disposals, and a number of other potential sources. Many issues related to public health and safety are created when petroleum products leak into the subsurface environment. Contamination of ground water aquifers, creation of explosive hazards, degradation of utility lines are only a few examples. When a contaminant is released into soil, it seeps downward as well as spreads in the lateral direction.

Once leakage is detected, necessary steps must be taken to prevent further spreading of the contaminants as well as to remediate the region of contamination. Depending upon the level of contamination, the affected region can be divided into the following zones: unsaturated zone, capillary zone, and free hydrocarbon zone. Due to the fact that diesel fuel density is lower than that of water, a layer of free product can locate itself on top of the water table. If possible, it should be removed by pumping prior to any other remediation process. In the unsaturated zone, the contaminant is held within the pore spaces by capillary and adhesion forces. Under typical conditions of the subsurface systems, the contaminant in the unsaturated zone is immobile; such conditions are referred to as residual saturation.

A number of techniques such as excavation with on-site/off-site treatment or disposal, biological treatments, soil flushing, and soil venting are used for remediation of contaminated soil. Soil venting is an effective method for removing volatile organic compounds such as gasoline or diesel fuel. Additional techniques such as steam injection and in-situ heating have also been em-

* Samsung Motors Inc, #50, Kongse-Ri, Kihung-Eup, Yongin-City, Kyungki-Do, Korea, 449-900
** University of California, Los Angeles, Los Angeles, CA90024-1597, U. S. A.

ployed to increase the removal rate in certain conditions. Lingineni and Dhir (1992) show that heating the incoming air greatly increases the removal rate for chemicals of low volatility.

In this study, remediation of soil contaminated with diesel fuel has been studied experimentally and analytically. Heated air are induced through the one dimensional test section, which is filled with glass beads and contains residual saturation of diesel fuel. The effect of variation of air flow rate and inlet air temperature on the remediation rate are investigated. The computer model developed by Linginei and Dhir are used to predict the removal of contaminants from the soil.

2. Theoretical Formulation of the Problem

2.1 Model description

The equation describing the transport of a multi-component contaminant during soil venting has been developed by Linginei and Dhir (1992) and Fotinich, Joo and Dhir (1996). The energy equation is

$$(\rho c_p)_m \frac{\partial T}{\partial t} = k_m \frac{\partial^2 T}{\partial x^2} - (\rho c_p)_g V \frac{\partial T}{\partial x} - \sum_{k=1}^{N} m_k'' h_{fg,k} + m_k'' h_{fg,w} \quad (1)$$

where ρ is density, c_p is specific heat capacity, subscript m and g refer to composite porous matrix and gas phase, T is temperature, t is time, k is thermal conductivity, x is axis along the soil column, V is gas velocity, h_{fg} is latent heat of vaporization. Subscript k and w are kth component of contaminant and water, respectively. Equation (1) is used to obtain temporal and spatial variation of temperature in the test section. The main assumption is that the temperatures of the air and soil are the same at any given moment in time. The second term on the right hand side of the equation represents the enthalpy flux of gas. The third and the fourth terms describe the latent heat absorbed during contaminant evaporation and the latent heat released by water vapor condensing from the incoming air. Effective thermal conductivity of the medium in the test section is

$$k_m = k_s \varepsilon_s + k_l \varepsilon_l + k_g \varepsilon_g \quad (2)$$

where ε is volume fraction, and subscript s and l refer to solid phase and liquid phase, respectively. The effective specific heat is

$$(\rho c_p)_m = \rho_g c_{pg} \varepsilon_g + \rho_s c_{ps} \varepsilon_s + \rho_l c_{pl} \varepsilon_l \quad (3)$$

The initial and boundary conditions applicable for the energy equation are:

$$T(x, 0) = T_{amb} \text{ at } x_i \le x \le x_o \quad (4)$$

$$T(0, t) = f(t) \text{ at } t > 0 \quad (5)$$

$$k_m \left(\frac{\partial T}{\partial x} \right)_{x_o, t} = 0 \text{ at } t > 0 \quad (6)$$

where T_{amb} is the initial temperature of the soil, and x_i and x_o are axial locations of the inlet and outlet of the test section, respectively.

One-dimensional vapor phase transport of each individual component on the contaminant in the test section can be described as

$$\rho_g \left[\frac{\partial C_{k,g}}{\partial t} + V_x \frac{\partial C_{k,g}}{\partial x} \right] = h_m A_l (C_{k,sat} - C_{k,g}) \quad (7)$$

for $k = 1, 2, \cdots, N$ where N is the number of components, where $C_{k,g}$ and $C_{k,sat}$ are the mass concentrations of the kth component of the contaminant in gas phase and saturation concentration, respectively, h_m is the mass transfer coefficient, A_l is specific surface area. Vapor diffusion in the x-direction is not included in the equation, since it is negligible in comparison with the bulk motion of vapor. The right-hand side expression in Eq. (7) describes the evaporation rate of contaminant inside the pore spaces. At irreducible saturation the contaminant is believed to exist in the form of pendular rings (Rose, 1958). Hence the mass transfer coefficient h_m can be determined from the correlations for mass transfer in packed beds of cylindrical pellets. Rose calculated the volumes and surface areas of pendular rings existing at the point of contacts of uniform size spheres. Using his results and assuming that the spheres are arranged in cubic fashion, the specific surface areas of these pendular rings can be calculated as a function of the liquid saturation. The applicable initial and boundary conditions are

$$C_{k,g}(x, 0) = C_{k,sat} \text{ for } x_i \le x \le x_o \quad (8)$$

$$C_{k,g}(x_i, t) = 0 \text{ at } t > 0 \quad (9)$$

For the liquid phase the similar equation can be written as

$$\rho_g\left[\frac{\partial C_{k,l}}{\partial t}\right]=-h_m A_l(C_{k,sat}-C_{k,g}) \tag{10}$$

for $k=1, 2, \cdots, N$ where the initial condition is

$$C_{k,l}(x, 0)=C_{k,l} \text{ for } x_0\leq x\leq x_i \tag{11}$$

Saturation concentration of pure kth species can be found from Raoult's law: $C_{k,sat}=y_k C_k^*$ for $k=1, 2, \cdots, N$. Assuming that the air phase behaves as an ideal gas, the ideal gas law can be used to find the vapor concentration of the pure species: $C_k^*=\frac{w_k}{RT}p_k^*$ where w_k is the molecular weight of kth species, R is the universal gas constant, and p_k^* is the saturation vapor pressure of the kth component.

2.2 Vapor pressure

Saturation vapor pressure of each component is important data for the analysis of soil venting. Frost, Kalkwarf, and Thodos made a correlation for many components in the form (Reid *et al.*, 1987)

$$\ln P_v=A-\frac{B}{T}+C\ln T+\frac{DP_v}{T^2} \tag{12}$$

where P_v is a vapor pressure in bars, A, B, C, and D are empirical constants. This equation is used to determine the component concentrations in the vented air as well as the amount of liquid contaminant remaining in the test section as a function of position and time. A finite difference formulation are used to solve the model equation. Given the initial liquid saturation values and the composition of the contaminant, the remediation times can be calculated for a given soil venting system configuration.

2.3 Chemistry of diesel fuels

According to the definition in the U. S. Chemical Substances Inventory, diesel fuel is a complex combination of hydrocarbons produced by the distillation of crude oil. It consists of hydrocarbons having carbon numbers predominantly in the range of C_9-C_{20} and boiling points in the range of approximately 163-357°C (Millner *et al.*, 1992).

Diesel fuel No. 2 or automotive and railroad diesel fuel contains normal and branched chain alkanes (paraffins), cycloalkanes (naphthenes), and aromatic and mixed aromatic cycloalkanes. It spans a carbon number range of C_7 to C_{20}. Diesel fuel is composed of a large number of components, many of which are not identified. Therefore, it is impossible to analyze each component separately when an attempt to investigate the soil venting process is undertaken. Mackay (1988) suggested a method to solve this problem, which was grouping hydrocarbons of similar properties. The components of similar volatility or vapor pressure as indicated by position on the capillary column gas chromatogram are grouped into normal alkanes. The C_8 hydrocarbon class consists of n-octane and all subsequent peaks up to, but not including C_9 (n-nonane). Since the saturation vapor pressure decreases with the growth of the carbon number, the average vapor pressure of the C_8 hydrocarbon class is smaller than that of n-octane.

It should be noted, however, that although the gross characteristics of diesel fuel are similar, its composition varies from manufacturer to manufacturer. Griest *et al.* (1986) presented a table comparing six different fuels of several manufacturers. It is noted that the mass fraction of some hydrocarbons varied significantly and some heavier hydrocarbons do not even exist in some diesel fuels. Therefore, it is important to analyze a particular diesel fuel used in the experiments in order to obtain accurate results.

3. Experimental Apparatus and Procedure

3.1 Soil venting experiment

In order to investigate the soil venting process and to verify the model, experiments were conducted in a transparent acrylic cylindrical tube with a length of 30cm, inside diameter of 114mm, and wall thickness of 6. 3mm. The test section was filled with 360 μm diameter glass beads up to a height of 220mm, leaving 80mm unfilled at the top. High temperature CPVC flanges were

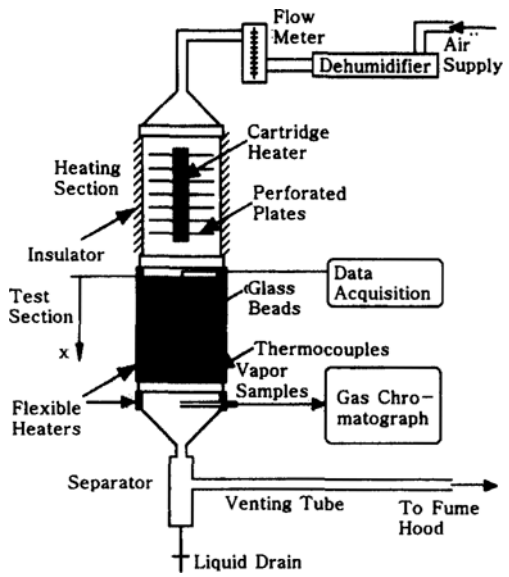

Fig. 1 Schematic of the experimental apparatus.

attached at the both ends of the pipe so that the main heater could be readily attached and detached. four omegalux silicone rubber fiberglass insulated flexible heaters were attached by means of metal clamp to the outer surface of the test section to prevent heat loss to surroundings. A schematic of the experimental apparatus is shown in Fig. 1.

Residual saturation created in the test section was measured using a gamma densitometer with 150-mci Cesium-137 source and Nal detector, both encased in lead. The source and the detector were mounted on a base plate which could be traversed in vertical direction along the test section. Gamma rays, emitted by the source, were attenuated through the test section, and were absorbed by the detector. A TN-7200 Multichannel Analyser was used to measure and display the attenuation counts. Measurements were performed for the test section filled with dry beads first, then for the section saturated with diesel and finally for the test section with residual saturation in it. Three sets of attenuation counts were obtained. The glass beads porosity as well as residual saturation in the test section were calculated with the use of the attenuation counts and logarithmic equations and were included in the computer program. Detailed information is in Fotinich's work (1997). The average soil porosity was about 0. 39 and diesel residual saturation was about 0.10.

Air was supplied from the pressurized air source and its flow rate was controlled and measured with a Dwyer air flow meter connected at the outlet of the air source. In order to remove moisture in the air stream, a filter and a 101mm diameter and 2 m long PVC pipe filled with calcium sulfate were installed on the line before air entered the flow meter. The dried air passed through the heating section. The heating section was of the same dimensions as the test section and had 20 cm long rod heater located vertically along the axis. Nine circular aluminum perforated plates were press fitted around the rod heater to increase the heat transfer area. Then the heated air entered into the test section. The pressure at the air inlet to the test section was about the ambient pressure. Pressure drop across the test section was negligible. At the bottom of the test section, a separator separated liquid and gas/vapor. The liquid was collected while the hydrocarbon vapor mixture was channeled to a venting hood.

Twelve K type thermocouples were mounted on a plexiglas rod with 2 cm distance. The rod was placed along the axis of the test section for the temperature measurements. Twelve more thermocouples were attached on the inner wall of the test section to provide the data for temperature distribution. An ACRO 900 data acquisition system was used to record the temperature. Measurements were displayed and stored using an IBM-PC.

In the experiment diesel fuel was used as the only contaminant. Initially, the test section was saturated with the fuel, which was then allowed to drain out for a substantial period of time. A small pressure was applied to the top of the test section to facilitate the drainage. The procedure was assumed to provide the residual saturation in the test section. Average values of porosity and residual saturation were calculated with the use of the Multichannel Analyser readings for the measurements taken at several locations along the test section.

Air flow rate was fixed at a given value and the air was passed through the main heating section. Once the air temperature at the exit of the main heater became steady and was about 5 °C higher than the desired venting air temperature, the main heating section was attached to the test section and the experiment was started. At the same time a flexible heater, attached to the outer surface of the test section and located above the other heaters, was switched on. The power input to the heater was controlled in order to achieve uniform temperature distribution at any given soil cross section. Following the high temperature front movement to the lower portions of the test section, the heaters were switched on one by one. Temperatures in the test section were recorded every 15 seconds by the data acquisition system. Gas/vapor samples were taken at regular time intervals from the sampling port employing heated air-tight syringes. The vapor samples in the syringes were processed with the help of Gas Chromatograph system, and the mass fraction of each component was analysed. The uncertainty of mass fraction is expected to be less than $\pm 16\%$.

3.2 Diesel fuel analysis

Prior to starting the experiments, diesel fuel No. 2, purchased at a gas station, was to be analyzed with the help of a Gas Chromatography system. Similarly to the approach proposed by Mackay (1988), diesel fuel was assumed to be composed of normal alkanes ranging from C_7H_{16} to $C_{20}H_{42}$. Each of the fourteen components is not just a normal alkane, but is the group, consisting of a large number of complex compounds. It could be assumed, however, that each group could be assigned the average property of a hydrocarbon known to be present in the group. The hydrocarbon classes are the groups of similar volatility as indicated by position on the capillary column gas chromatogram.

Table 1 is the composition of diesel fuel used in the experiment. The uncertainty of the presented result is calculated to be less than $\pm 12\%$. It can be noted that composition of diesel fuel used in the experiment differs significantly from the one proposed by Mackay. Therefore, the composition of diesel fuel should be carefully examined in order to acquire proper mass balance.

Table 1 Experimentally estabilished composition of diesel fuel used in the experiment.

Carbon No.	Mass fraction (%)	Volume fraction (%)	Mass fraction proposed by Mackay (1988)
7	0.62	0.69	0.06
8	0.23	0.26	0.10
9	0.40	0.43	0.26
10	3.54	3.70	2.58
11	12.18	12.55	6.80
12	15.33	15.62	9.15
13	14.26	14.38	14.17
14	11.64	11.67	13.75
15	8.48	8.40	12.39
16	7.06	6.97	12.39
17	5.97	5.85	11.45
18	4.94	4.82	9.29
19	3.93	3.81	4.79
20	3.44	3.32	2.82
21	2.50	2.39	0
22	1.82	1.73	0
23	1.35	1.27	0
24	0.93	0.87	0
25	0.51	0.48	0
26	0.42	0.39	0
27	0.22	0.20	0
28	0.14	0.13	0
29	0.05	0.04	0
30	0.04	0.03	0
Totals	100	100	100

4. Results and Discussion

Three soil venting experiments were conducted. The first one had venting air flow rate and temperature set to 330 cm^3/s and 90 °C, respectively. The second experiment had the venting air flow rate decreased by the factor of three which result-

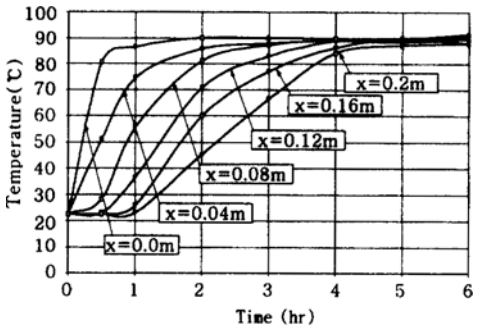

Fig. 2 Temperature variation in the test section with time for the first experiment (Q_{air}=330 cm³/s, T_{inlet}=90°C).

ed in 110 cm³/s, while the temperature was kept the same (90°C). The third experiment was conducted with the venting air temperature decreased to 60°C, while the air flow rate was 330 cm³/s. The initial temperature in the test section for all three cases was about 23°C.

4.1 Soil venting of air flow rate of 330 cm³/s and inlet temperature of 90°C

The temperature variations along the axis of the test section with time for the first experiment are shown in Fig. 2. At the first moment of time, the temperature at all positions was close to the initial temperature. The fastest rise in the temperature occurred at the inlet surface of the glass bead packing, where the inlet temperature reached the steady state temperature of 90 ° C in about 2 hours. Temperatures at all locations gradually increased until they reached the steady state value which happened at about 5 hours from the beginning of the experiment.

The effluent vapor composition at the exit of the test section was measured. It is noted from Fig. 3, which is typical for this experiment, that only a few components of the diesel fuel exits in the effluent air at any given time. For example, it can be said that C_7-C_8 hydrocarbon classes are removed completely from the soil column within 2 hours from the beginning of the experiment. Also, the C_{10}-C_{16} hydrocarbon classes are being removed, with the peak mass fraction belonging to C_{11} class. The remaining C_{18}-C_{20} hydrocarbon classes have not yet started to evaporate. A simi-

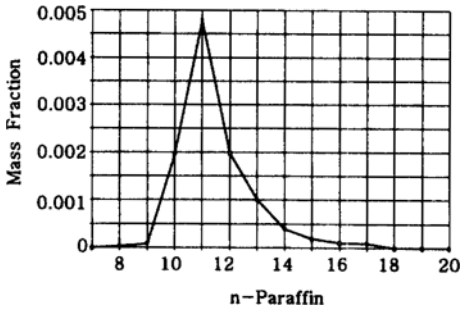

Fig. 3 Composition of effluent vapor at 2 hours (Q_{air}=330 cm³/s, T_{inlet}=90°C).

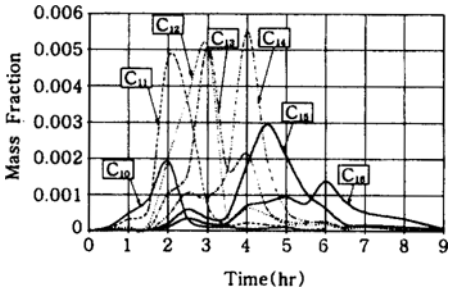

Fig. 4 Mass fraction of selected hydrocarbon classes vs. Time in the effluent air (Q_{air}=330 cm³/s, T_{inlet}=90°C).

lar behavior in the composition of the effluent gas/vapor mixture was observed at other times, i. e. some species being already removed, some species continuing to be removed, and some species yet to evaporate.

Mass fraction variation with time for seven hydrocarbon classes are presented in Fig. 4. All experimental curves have similar trends. For most of the curves there is an initial growth of the mass fraction till it reaches the maximum value. After passing the maximum value the mass fraction decreases rapidly and then decreases slowly until the component is removed completely. Also, it is evident that the diesel components are removed one by one according to their volatilities with higher volatile components being removed first. It can also be noted that the maximum of the curves shifts with time towards the heavier hydrocarbon classes.

4.2 Effect of flow rate variation

The temperature variation in the test section for

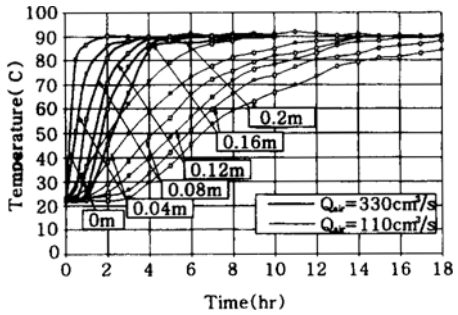

Fig. 5 Temperature variation in the test section with time for experiments with different flow rates.

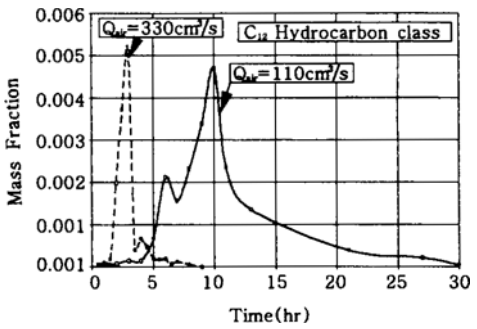

Fig. 6 Mass fraction of C_{12} hydrocarbon class in the effluent air as a function of time for experiments with different flow rates.

the experiment with air flow rate of 110 cm^3/s are plotted with that for the air flow rate of 330 cm^3/s in Fig. 5. The inlet air temperatures of both experiments equal to 90°C. It is clearly seen that temperature rise in the test section depends strongly on the air flow rate. For example, at the top surface of the soil the temperature reaches 90°C after 2 hours from the beginning of the experiment at higher flow rate, whereas it takes about 9 hours for the lower flow rate. Also, for the bottom region of the test section it takes about 5 hours to heat up to about 90 ° C in the experiment with higher flow rate, whereas it takes longer than 18 hours for the lower flow rate. The rate of enthalpy input to the test section depends directly upon the value of the air flow rate. For the lower flow rate and same inlet temperature, the energy input in the test section is three times less than that for the higher flow rate. Thus, it takes much longer to heat up the glass beads filling the test section to the steady state temperature.

The mass fraction variation of C_{12} hydrocarbon class in the effluent air as a function of time for the both experiments is shown in Fig. 6, which is typical for this experiment. The curve for lower flow rate shows similar shape with that for higher flow rate, while the peak is more wider in lower flow rate. The peak for lower flow rate is shown 7 hours later than that for higher flow rate. The gap between two peaks increases significantly for the heavier hydrocarbons. Hence, venting air flow rate affects the heavier components the most.

The other interesting phenomenon may be reported by noting that for most of the components the maximum mass fractions are lower for the experiment with lower air flow rate. For example, maximum mass fraction of C_{12} hydrocarbon class is about 0.0052 for the experiment with higher flow rate, while it is about 0.0047 for the experiment with lower flow rate. The difference between two peaks is more significant for the heavier hydrocarbons. As is stated by Raoult's law, mass fraction of a component in gaseous phase above multi-component liquid contaminant is proportional to mass fraction of the component in liquid phase. Since the removal process of the diesel component is slowed down for the experiment with lower flow rate, larger amount of components lighter than C_{12} remain in liquid phase when the amount of C_{12} hydrocarbon class reaches its maximum in about 10 hours from the beginning of the experiment. Thus, the maximum mass fraction of C_{12} in gaseous phase is considerably lower in the experiment with the lower flow rate in comparison to the experiment with higher flow rate.

4.3 Effect of inlet temperature variation

The temperature variation in the test section with time for the experiment with air flow rate of 330 cm^3/s with inlet temperature of 60 ° C is shown in Fig. 7 with the result for inlet temperature of 90°C. For the same air flow rate, the temperature distribution in the test section and propagation of thermal fronts show a similar pattern. The surface temperature of the soil reaches the inlet air temperature about 2 hours for

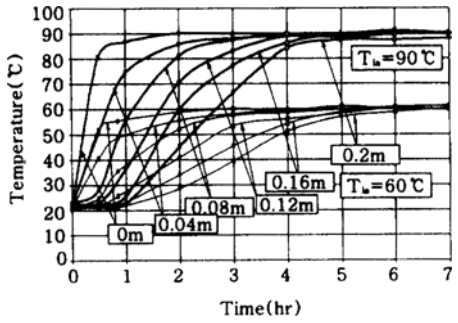

Fig. 7 Temperature variation in the test section with time for experiments with different inlet air temperature.

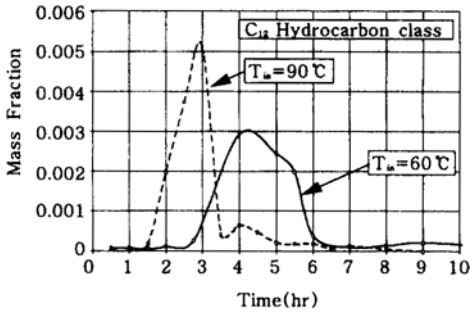

Fig. 8 Mass fraction of C_{12} hydrocarbon class in the effluent air as a function of time for experiments with different inlet air temperature.

both experiments. The bottom of soil reaches the inlet air temperature about 6 hours later for both experiments.

Figure 8 shows the mass fraction of C_{12} hydrocarbon class in the effluent air as a function of time for the experiments of both inlet air temperatures. The curves of mass fraction versus time show similar trend to that discussed in the previous section. However, the removal process for the individual components behaves in a different manner in comparison to the experiments with different air flow rates. For the experiments of low inlet air temperature, the maximum value of mass fraction is considerably lower while the time shift in the curves of the mass fraction is less pronounced. This happens due to the fact that vapor pressure of the hydrocarbons notably decreases with temperature. The decrease in the maximum mass fraction of a component in the

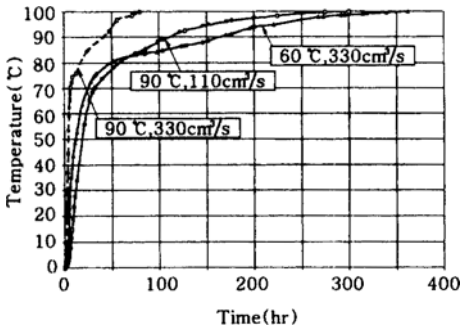

Fig. 9 Effect of venting air flow rate and temperature on the contaminant removal history.

effluent air causes the increase in removal time of the component. Therefore, despite the fact that the shift in time for peak to occur is not very long, it takes significantly longer to completely remove a particular component. Hence, it takes much longer to remove all of the hydrocarbons completely.

4.4 Time for complete clean up

Soil venting experiments with the inlet air temperature of 90°C and 60°C and air flow rates of 330 cm^3/s and 110 cm^3/s were conducted to find time periods necessary to fully remove contaminant from the test section. Curves representing percentage of contaminant removed versus time are shown in Fig. 9. For the venting air with the highest inlet temperature and highest flow rate it takes about 80 hours to remove residual diesel from the test section. When either air flow rate or the inlet air temperature is decreased, the time periods necessary to fully remove the contaminant significantly increase to 300 hours and 360 hours, respectively. So, 30 ° C increase in temperature of incoming air allows to decrease the clean up time by a factor of 4.5, while the threefold increase in air flow rate reduces the clean up time by a factor of 3.75. Thus, with a moderate temperature increase the achieved reduction in the clean up time is higher than for considerable increase in air flow rate.

The curves for experiments with lower temperature and with lower flow rate cross each other in about 70 hours in Fig. 9. Prior to this time, the overall contaminant removal rate for the lower inlet temperature is higher than that for the lower

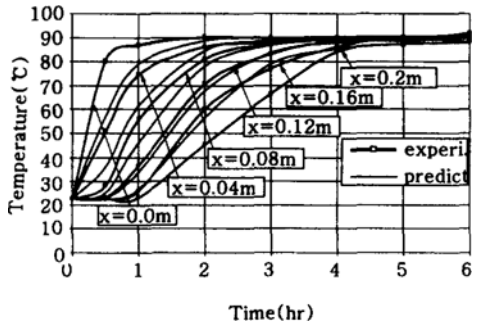

Fig. 10 Experimental and predicted temperature variation in the test section for the first experiment.

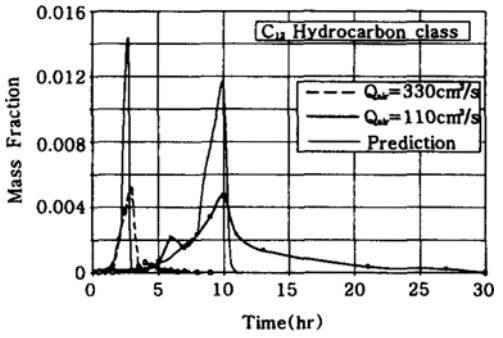

Fig. 11 Experimental and predicted mass fraction of C_{12} hydrocarbon class as a function of time for the different flow rates.

air flow rate. After 70 hours, the overall contaminant removal rate for the lower air flow rate is higher than that for the lower inlet temperature and shows the complete clean up achieved in less time. The components lighter than C_{16} are removed completely in 70 hours from the beginning of both experiments. Thus, only the components heavier than C_{16} still remain trapped in the test section and they are the ones most affected by the inlet air temperature decrease. Therefore, the heating of the incoming air is especially important for the heavy components. Also, it can be said that for the short time intervals the process is flow rate dominated, while for long periods it is observed to be temperature dominant.

4.5 Comparison of model predictions with the experiments

Experimental and predicted temperature distributions for the experiment with the venting air flow rate of 330 cm^3/s and inlet air temperature of 90 ° C are presented in Fig. 10. Curve for predicted temperature at the top of the soil ($x=$ 0.0 m) coincide with the experimental curve because the experimental temperature variation at the top of the soil are used in the computer program. It can be noted from the figure that the experimental and predicted temperatures are in general agreement, although the predicted temperatures are higher than the experimental temperatures especially at the bottom of the soil. For the experiments with different flow rates and with different inlet air temperatures, the experimental and predicted temperatures are in general agreement also.

Comparison between the experimental and predicted mass fractions of C_{12} hydrocarbon classes as a function of time for the experiments with two different flow rates is presented in Fig. 11, which is typical for this experiment. The experimental and predicted values are in general agreement. However, the peaks of predicted mass fractions are higher than the experimentally obtained values. Also, the complete removal times of all the components are underpredicted. The model predicts complete removal of C_{12} hydrocarbon classes in 2.7 hours for the experiment with flow rate of 330 cm^3/s, but the complete removal in the experiment is considerably delayed. One possible reason for the difference in behavior between model predictions and data is that, in the present model, the contaminant species which remaining in the liquid are assumed to be mixed completely at every time step. In reality, however, the contaminant species, which present in the inner layers, must diffuse out to the interface. Hence, the predicted peaks are higher than the experimental ones and the predicted species concentration in effluent gases drops off rapidly. However, the prediction for the removal of total diesel trapped in the test section is in good agreement with the experimental data within the uncertainty of experiment, $\pm 16\%$, although the agreement between the prediction and data for the single component is not perfect.

5. Conclusion

Laboratory experiments to remediate the soil contaminated with fresh diesel fuel were performed in a one-dimensional test section. Diesel fuel was modeled similarly to the group approach proposed by Mackay (1988). It is observed that the diesel fuel components are removed according to their volatility. Lighter diesel components, which have higher volatility, are removed first. An increase in venting air flow rate or inlet air temperature can considerably speed up the process. Although the increase in inlet air temperature does not significantly affect the removal rates of the lightest hydrocarbons, it is found to be very effective in increasing removal rate of the heavier components. It is also observed, that at early time periods the venting process is flow rate dominant, while at long time periods it is temperature dominant.

A one-dimensional, non-isothermal, complete mixing model is used to predict evaporation rates of the contaminant components and temperature distribution in the test section. Model results have been found to be in agreement with the experimental data. It is noted that, since species diffusion within the liquid contaminant is not included in the model, the predicted magnitudes of peak concentrations in exiting gases are higher and the drop in concentration is faster than for the experimental results.

References

Fotinich, A., 1997, "Experimental Investigation of Remediation of Soils Contaminated With Diesel Fuel," Master of Science Thesis, University of California at Los Angeles, CA, U. S. A.

Fotinich, A., Joo, Y. and Dhir, V. K., 1996, "Investigation of Remediation of Soil Contaminated with Diesel Fuel Using Air Venting," *Proc. International Mechanical Engineering Congress and Exposition,* Atlanta, Georgia, Nov. 17~22.

Griest, W. H., Higgins, C. E. and Guerin, M. R., 1986, "Comparative Chemical Characterization of Shale Oil-and Petroleum-Derived Diesel Fuels," *CONF-851027-5.*

Lingineni, S. and Dhir, V. K., 1992, "Modeling of Soil Venting Processes to Remediate Unsaturated Soils," *Journal of Environmental Engineering.* Vol. 118, pp. 135~152.

Mackay, D., 1988, "The Chemistry and Modeling of Soil Contamination with Petrolium," in *Soils Contaminated by Petroleum: Environmental and Public Health Effects* (Edited by Calabrese, E. J., Kostecki, P. T. and Fleischer, E. J.), John Wiley & Sons, New York.

Millner, G. C., Nye, A. C. and James, R. C., 1992, "Human Health Based Soil Cleanup Guidelines for Diesel Fuel No. 2," in *Contaminated Soil-Diesel Fuel Contamination* (Edited by Kostecki, P. T. and Calabrese, E. J.), Lewis Publisher, Boca Raton.

Reid, R. C., Prausnitz, J. M. and Poling, B. E., 1987, *The Properties of Gases and Liquids,* 4th edition, McGraw-Hill, New York.

Rose, W., 1958, "Volumes and Surface Areas of Pendular Rings," *Journal of Applied Physics,* Vol. 29, No. 4, pp. 687-691.